Journal of Theoretical and Applied Information Technology
15th November 2025. Vol.103. No.21

ISSN: 1992-8645 www.jatit.org E-ISSN: 1817-3195

AN ENHANCED EDGE PRESERVING TECHNIQUE FOR MULTIFOCUS IMAGE FUSION

VAKAIMALAR ELAMARAN[1], RAMYA R[2], ANANDH A[3],

PRAVEEN KUMAR PREM KAMAL[4], DEEPA PRIYA V[5]

[1]ASSOCIATE PROFESSOR, Department of Information Technology, Kamaraj College of Engineering and Technology, India

[2] ASSOCIATE PROFESSOR, Department of Computer Science and Engineering, Kamaraj College of Engineering and Technology, India

[3]ASSOCIATE PROFESSOR, Department of Computer Science and Engineering, Kamaraj College of Engineering and Technology, India

[4]ASSOCIATE PROFESSOR, Department of Artificial Intelligence and Data Science, Kamaraj College of Engineering and Technology, India

[5]ASSISTANT PROFESSOR, Department of Information Technology, Kamaraj College of Engineering and Technology, India

E-mail: [1]vakaimalarit@kamarajengg.edu.in, [2]ramyacse@kamarajengg.edu.in, [3]anandhcse@kamarajengg.edu.in, [4]praveenads@kamarajengg.edu.in, [5]deepapriyakcet@gmail.com

ABSTRACT

Image fusion aims to combine complementary and repetitive information present in multiple images of the same scene that has been captured by different cameras or sensors and generates a single image with improved quality. This work proposes an algorithm for fusing multifocus images using edge superimposition and Dense Scale Invariant Feature Transform (Dense SIFT). Due to the depth of the field, when background is focused, boundary between the background and expanded foreground objects become unclear and vice versa. To overcome this, edge superimposition is applied to enhance the boundary region between the foreground and background objects. As an initial step, edges are detected from a source image using sobel operator and the extracted edge features are superimposed on the next source image and vice versa. This step plays a vital role in the proposed approach, since sharpness of the edges is crucial in the picturesque quality of the image. After super imposition of edges, Dense SIFT descriptor extracts features at every pixel and helps in deciding the resultant pixels in the fused image. The image feature-based metrics such as Average Gradient, Edge Intensity, Standard deviation and Spatial Frequency demonstrates the superior ability of the proposed algorithm in preserving edges compared to numerous other algorithms under consideration.

Keywords: *Dense SIFT, Feature, Image fusion, Multifocus, Superimposition.*

1. INTRODUCTION

An image taken in a specific scene might lack certain details, whereas two separate images capturing the same scene may have different information. Image fusion combines complementary and redundant information from multiple source images to enhance and elevate the overall quality of the image [1]. The fused image incorporates all the necessary information from the source images and is highly informative.

Image fusion enhances the source images and generates a single image for further processing in application areas such as medical imaging for improved diagnosis, satellite imagery for enhanced analysis, surveillance systems for better object detection and recognition, remote sensing for improving the accuracy of land cover classification and change detection, concealed weapon detection and battle field monitoring for facilitating more effective threat detection and response etc.,

The source images used in image fusion may be multiview, multiexposure, multifocus, multitemporal or multimodal images. Multitemporal images are the images captured at different times and multiexposure images are acquired with different lighting conditions. Multimodal images are images with different modalities such as CT and MRI, visible and infrared, multispectral and panchromatic [2]. Multiview images are images acquired at different angles and multifocus images are the images captured from a singular viewpoint, ensuring

consistency in the perspective of the scene, but with different focus.

There are situations in which source images are misaligned. The reason may be due to geometries, positions and rate of capture of the sensors. One image might represent a subset of other and might have been acquired with different sensors or at different angles. Registration aligns the source images by matching the spatial correspondence between the images. Registered images are considered in this work.

An efficient image fusion algorithm should be capable of extracting all essential data from the source images and replace missing information [3]. It should remove noise, but should not introduce any artifact such as blocky or ghost effect.

2. RELATED WORK

This section discusses the traditional and recent multifocus image fusion techniques and the metrics that can be used for evaluating the efficiency of the algorithms.

2.1 Traditional Multifocus Image Fusion Methods

Traditional algorithms for image fusion can be broadly categorized into spatial domain and frequency domain. In frequency domain, fusion is done after down sampling the source images whereas there is no down sampling in the spatial domain. Hence the frequency domain techniques are termed as multiscale and the spatial domain techniques are called as single scale [4].

Image manipulation is done with respect to each and every pixel in the spatial domain. It enhances the images by using smoothening and sharpening filters. Image fusion techniques are categorized under pixel-based, block based or region-based. Every pixel in the source image is considered for choosing the resultant pixel in the fused image in pixel level fusion. Since every pixel is considered, pixel level fusion sharpens the image, enhances the features, substitutes missing data and replaces faulty data [5].

In many scenarios, the essential and necessary features cannot be retrieved from a single pixel. Hence block based methods which processes the images in blocks are proposed. In block based approach, decision is made based on the neighbouring pixels [6]. Even though this approach improves the convergence between each pixel, it introduces blocky effect if the chosen block size is incorrect. The size of the block should be nominal. In region-based fusion, processing is done in regions rather than pixels. It focuses on Region Of Interest (ROI) and each pixel in the ROI is taken into consideration [7], [8]. Segmentation generates set of regions and extract boundaries, distinct colour areas, edges, corners, textures etc., for further analysis or processing. The focus level of the segmented regions is compared and the best-focused regions are combined to get the resultant image [9].

In the frequency domain, original images are decomposed into different components based on their frequency content - low, median and high frequencies. These individual components are later combined by using specific weighted average, aiming to emphasize details while retaining the essential information of the original image to perform image fusion and enhancement [10].

Some of the frequency domain techniques are Discrete Wavelet Transform [11], [12] Discrete Cosine Transform [13], Dual Tree-Complex Wavelet Transform [14], Non Subsampled Contourlet Transform, Stationary Wavelet Transform [15], Multiscale Singular Value Decomposition [16], Guided Filter [17], Support Value Transform [18], Discrete Cosine Harmonic Wavelet Transform [19]. Fusion is done on the decomposed images using some fusion guidelines and finally inverse transform is applied to obtain the resultant image [20]. Fusion rule should be designed with care to avoid unexpected information loss.

2.2 Recent Multifocus Image Fusion Methods

Nowadays, deep learning is employed to Multi Focus Image Fusion (MFIF) and there is vast increase in the use of deep learning techniques. Liu et al. [21] introduced the first Convolutional Neural Network (CNN) which is not only used for extracting the features but also used in the task of classifying fusion rules. The score map is generated by passing input source images to the pre-trained CNN model. After that nearly forty MFIF algorithms based on deep learning techniques are introduced by researchers.

MFIF algorithms, based on deep learning techniques, are classified either as supervised or unsupervised. Supervised algorithms necessitate a substantial volume of training data accompanied by ground-truth annotations to effectively train the

model. Some of the supervised MFIF algorithms are multi-level deeply supervised CNN [22], pixelwise convolutional neural network [23], multi-level features convolutional neural network [24], a common CNN based framework [25].

MFIF methods based on supervised learning require an extensive amount of training data that is labeled. This process demands a considerable amount of human effort and time. Unsupervised MFIF algorithms resolve this issue. The researchers have proposed the unsupervised MFIF algorithms which incorporated MFNet [26], encoder-decoder network [27], DIF-Net [28] and FusionDN [29].

The generative model focus on merging or fusing images aiming to minimize any distortions in both spectral (related to frequency content) and spatial (related to position or location) domains [30].

2.3 Metrics for Evaluation

The effectiveness of any image fusion algorithm can be assessed through two primary evaluation methods: subjective, focusing on qualitative aspects and objective, emphasizing quantitative measurements [31]. Subjective evaluation involves human observers assessing the visual quality of the fused image. However, as each observer might have their own individual standards or preferences when observing these images, subjective evaluation can introduce variability in the assessment process. This in turn leads to biased evaluation and hence relying solely on qualitative evaluation might not suffice. Therefore objective assessment metrics are also essential. They are the metrics derived from information theory, image features, similarity of the structure and human perception.

Image feature based metrics measure the efficiency of transferring features from the input images to the resultant image. It includes Gradient-Based Similarity measurement (QAB/F), Phase Congruency (Qp), Average Gradient (AG), Spatial frequency (SF), Edge Intensity (EI), Standard Deviation (SD).

The metric QAB/F quantifies the information about edges that are present within the fused image. i.e., edge strength and orientation preservation from source input images to the resultant image. Phase congruency provides an absolute measure of feature using the principal moments which contains corners and edges information. AG calculates all the texture features and some extent of detail features of the resultant image. SF calculates the general activity level of the space in the image. EI measures the edge compactness which reflects the local density of network edges. SD finds out the contrast present within the resultant image.

Scale Invariant Feature Transform (SIFT) descriptor establish matches in the content of the images which are different in translation, rotation and scale parameters. Local features in images and feature descriptors are widely applied in numerous computer vision applications such as object recognition and image registration. The most prevalent SIFT algorithm which includes identification and characterization of distinctive features was proposed by [32]. Feature descriptors are generated for all interest points by capturing and analysing the details of local gradient. SIFT is rotation and space invariant. It is sparse feature representation, as it generates feature descriptors for interest points only.

Dense SIFT is an extension of SIFT descriptor. But there is no feature detection stage for selection of interest points, since Dense SIFT generates feature vector for all pixels. Dense SIFT involves transforming the image into feature space for enhanced detection of active features, and subsequently, merging these features based on a fusion strategy before converting back to image space.

In [33], the authors used sum of the feature vectors as the activity level measurement. Initially, classification maps are generated, categorizing pixels as focused, defocused or uncertain. These maps form the basis for the initial decision map. Further refinement involves fine-tuning the pixels that are uncertain by utilizing frequency in the spatial domain for classification. But in the proposed work, each and every element in the feature vector of corresponding pixels in the input images is compared and fusion is done.

.

3. METHODOLOGY

The proposed Multifocus Image Fusion using Edge superimposition and Dense SIFT (MIFED) algorithm is classified under spatial domain technique. The framework of the proposed MIFED approach is depicted in Fig. 1.

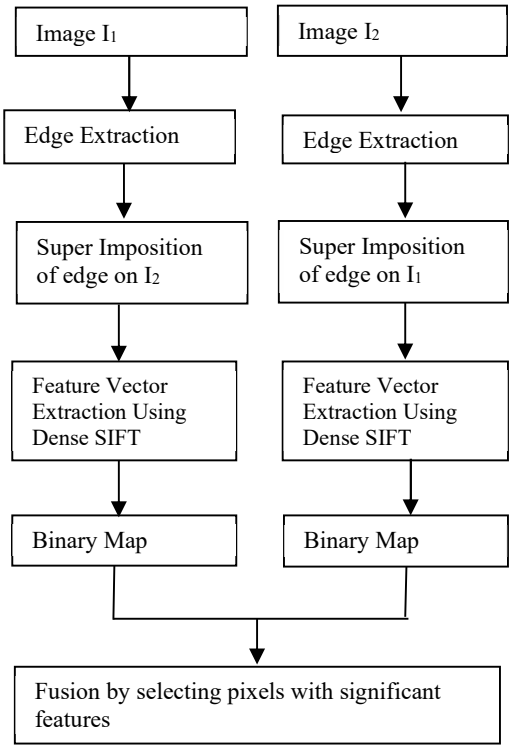

Figure 1: Framework of the MIFED Algorithm

The main contributions of the work are as follows:

- Edge superimposition is employed which enhances the boundary between the focused and unfocused regions and reduces the defocus spread effect.
- Fusion is achieved by considering each element in the Dense SIFT feature vector of corresponding pixels in the input images.
- Utilizes a combined approach of pixel and feature-based fusion, leveraging the strengths of both methods.

3.1 Edge Extraction

In order to enhance the edges, edge detection should be done first. Edges are detected by applying various mathematical methods which identifies the points in the image where there is sharp change in the brightness. Some of the techniques used for edge detection are canny, prewitt and sobel.

The sobel operator is resistant to noise when compared to prewitt operator because sobel is the combination of differentiation and Gaussian smoothing. Sobel operator estimates the direction of the edge along with the magnitude of the edge at a specific point. When applying Canny edge detector, the value of the two thresholds should be chosen with at most care. Otherwise, the edges will not be detected accurately. And also, Canny edge detection consumes more time because it involves complex computation which is not in the case of Sobel operator. The detection of edges along with their orientations is simple in sobel because of the approximation of the gradient magnitude in the cross operator. Hence sobel operator is chosen in the MIFED algorithm. The filters along the x direction (G_x) and the y direction (G_y) of the Sobel operator are given by

-1	-2	-1
0	0	0
1	2	1

G_x

-1	0	1
-2	0	2
-1	0	1

G_y

The value at the centre pixel Z_5 is given in equation (1).

$$\nabla f=|(Z_7+2Z_8+Z_9)-(Z_1+2Z_2+Z_3)|+|(Z_3+2Z_6+Z_9)-(Z_1+2Z_4+Z_7)| - \quad (1)$$

3.2 Edge Superimposition

The sharpness of edges in the image enhances the quality [34]. Hence in the MIFED algorithm, edges are extracted in one source image and super imposed on other source image. This superimposition is done on both images since there may be dissimilarity in edge information among the source images. This step reduces discontinuities in edges and enhances edges in both of the source images.

The steps in edge superimposition are

1. Extract edge information E_1 and E_2 from the source images I_1 and I_2 using sobel operator.
2. Superimpose the edge E_2 on the first image I_1 using weighted addition as in Eq.,(2).
   $I_{INTER}=W_1*I_1+W_2*E_2$ (2)
   where w1=(Average pixel value of I_1)/(Maximum pixel value of I_1) and $w_2=(1-w_1)*0.1$
3. Superimpose the intermediate image I_{INTER} on the second image I_2 using Eq.,(3).
   $I_{IMPOSE}=W_3*I_2+W_4*I_{INTER}$ (3)
   where w3=(Average pixel value of I_2)/(Maximum pixel value of I) and w4=1
4. Repeat steps 2 and 3 by considering I_2 as first image and I_1 as second image, edge as

Journal of Theoretical and Applied Information Technology
15th November 2025. Vol.103. No.21

ISSN: 1992-8645 www.jatit.org E-ISSN: 1817-3195

E_1 for superimposing edge details of I_2 on I_1.

The above steps replace any missing edge details in the source images I1 and I2 which in turn enhances the sharpness of the edges.

3.3 Feature vector Extraction

Dense SIFT descriptor extracts orientation information of individual pixel and generates a feature vector which serves as an activity level measurement that helps to decide the resultant pixels in the fused image. Image fusion attempt to incorporate the features detected from all the pixels in the original images which in turn improves the quality of the resultant image. Hence Dense SIFT, the dense feature representation which generates feature descriptor for all pixels is adopted in the MIFED algorithm. Dense SIFT is not rotation and space invariant but this feature does not affect the MIFED algorithm since preregistered images are supplied as source images.

Dense SIFT descriptor generates 1x128 feature vector for each pixel which contains the orientation information. In order to generate feature descriptors for boundary pixels, sources images are extended by filling with zero valued pixels. The MIFED algorithm makes use of sliding window technique during feature vector extraction. A neighborhood patch of 48x48 pixels is divided into 4x4 cell array for entire pixels in the source images. An orientation histogram for each cell array with 8 bins is constructed by calculating orientation and gradient magnitude. Each bin covers 45 degrees ranges from 0 to 360 degrees. Thus, a 1x128 (4x4x8) dimensional feature vector is generated for each pixel.

3.4 Fusion

Each and every value in the 1x128 feature vector generated for corresponding pixels in the source images is compared and if the value from the feature vector of first image is greater than second image, then 1 is assigned otherwise 0. This results in MxNx128 binary maps for a MxN image.

The binary map decides the resultant pixel in the fused image. If the number of 1s in the binary map is greater, then the pixel from the first image has more significant features than the pixel from the second image and hence the pixel from the first image is chosen for resultant pixel in the fused image.

Similarly, the corresponding pixel from the second image is chosen if the number of 0's is more in the binary map. This step is done for all MxN pixels which generates the fused image. The pseudocode of the MIFED algorithm is presented in the Algorithm 1.

Algorithm 1 MIFED

Input: I_1, I_2 Output: I_f
function MIFED(I_1, I_2)
$E_1 \leftarrow$ SOBEL(I_1)
$E_2 \leftarrow$ SOBEL(I_2)
$I_{2_IMPOSE} \leftarrow$EDGE_SUP_IMP(I_1, I_2, E_1)
$I_{1_IMPOSE} \leftarrow$EDGE_SUP_IMP(I_2, I_1, E_2)
$I_{2\_IMPOSE\_FEATURE} \leftarrow$ DENSE_SIFT(I_{2_IMPOSE})
$I_{1\_IMPOSE\_FEATURE} \leftarrow$ DENSE_SIFT(I_{1_IMPOSE})
$I_f \leftarrow$ FUSE($I_{1\_IMPOSE\_FEATURE}$, $I_{2\_IMPOSE\_FEATURE}$)
return I_f
end function
Explanation:
1. SOBEL(X) extracts the edge information from image X
2. EDGE_SUP_IMP(I_x, I_y, E_z) is given in Algorithm 1A
3. DENSE_SIFT(X) generates the feature vector for entire pixels in Image X
4. FUSE(X,Y) selects the pixels with most significant features

Algorithm 1A EDGE_SUP_IMP

Input: I_x, I_y
Output: I_y
function EDGE_SUP_IMP(I_x, I_y, E_z)
$w_1 \leftarrow$ Avgpixelof I_x/Maxpixelof I_x, $w_2 \leftarrow (1- w_1) * 0.1$
$w_3 \leftarrow$ Avgpixelof I_y/Maxpixelof I_y , $w_4 \leftarrow 1$
$I_{inter} \leftarrow w_1 * I_x + w_2 * E_z$
$I_y \leftarrow w_3 * I_y + w_4 * I_{inter}$
return I_y
end function

4. RESULTS AND DISCUSSIONS

The MIFED algorithm has been evaluated with real time data sets of gray scale as well as colour images. The algorithm has been implemented for all twenty image pairs in lytro dataset and average value of the feature based metrics - AG, EI, QAB/F, QP,

SD, SF are compared with existing methods [35] in Table 1 in Page no. 8 (Top three values are shown in Red, Green and Blue respectively).

The AG attained using the proposed MIFED is 9.966 whereas all the methods have less than 7 except SFMD with 8.153. Similarly, EI is 100.18 i.e., 29% greater than all other compared methods except SFMD with 84.40. The SD is 63.9905 whereas all other methods have SD lesser than 61.6 except MGFF with 63.218 and SFMD with 62.9955.

The SF for all methods is less than 20 and SFMD has 23.409. The SF attained using the proposed MIFED is 29.34 which is nearly 50% better than the compared methods. None of the algorithm will produce the best results for all the metrics and the same is the case for MIFED algorithm. The best QAB/F 0.7454 is produced by TF whereas MIFED has 0.7393. The phase congruency is 0.8194 produced by GFDF whereas MIFED has 0.7567.

The proposed MIFED algorithm has also been tested with the real world data set generated by S.Xu et al [36], J. Zhang et al [37] and H. Zhang [38]. In the first data set, the authors have generated 710 pairs of images and categorized 260 pairs of images as simple set and remaining 450 pairs as complex set based on the focus in the boundary regions. In the second dataset, the authors have provided set of 19 images, out of which 13 sets have two source images and remaining 6 sets have more than two source images. The third data set consists of 120 pairs of images.

The Figure 2 in page no. 9 shows some of the resultant fused images obtained using the MIFED algorithm along with the source images. All the images (a1) to (a6) are the source images focused on the foreground objects and the images (b1) to (b6) are the source images focused on the background. In the resultant fused images (c1) to (c6), both of the fore ground and background objects are clear.

While considering the monk image in the 6th row in the in Figure 2, it is observed that the water droplets are blurred and clear in (a6) and (b6) respectively. When it is observed carefully, it is evident that the boundary around the water droplets in the fused image in (c6) is enhanced even better than the source image shown in Figure (a6). The reason behind this enhancement is due to edge superimposition. The performance metrics for the set of images in Figure 2 is tabulated in the Table 2.

Table 2: Feature Based Metrics of MIFED algorithm for the images in Figure 2

Image	AG	EI	$Q^{AB/F}$	Q_p	SD	SF
Car	10.71	105.47	0.692	0.790	58.92	37.55
Chair	10.35	104.29	0.720	0.765	52.85	30.74
Moun-tain	18.32	165.65	0.741	0.647	50.47	48.18
Red Rose	6.65	69.76	0.709	0.823	40.62	15.64
Tea Cup	6.08	59.39	0.723	0.767	76.64	21.62
Monk	3.45	34.24	0.736	0.369	38.67	15.04

In the Figure 3 in page no. 10, A and B shows the source images and C to O shows the fused images obtained using Multi-scale weighted gradient-based fusion, Guided Filter, CNN, Iterative Fusion Convolution Network, unsupervised deep model, Dense SIFT, Cross Bilateral Filter [39], Convolutional Sparse Representation [40], Guided filter-based focus region detection [41], Multimodal Multiscale Fusion Network [42], Multi-scale Transform and Sparse Representation [43], Multi-scale Morphological Focus-Measure fusion [44], Booster Random Walks-Based Algorithm with two-scale focus maps [45] respectively.

The proposed MIFED algorithm's result is shown in Figure 3 (P). The background scenery comprises of numerous trees, a lawn and a river, while the foreground features a single flower. The source image 1 in Figure 3A focuses on foreground whereas the source image 2 in Figure 3B focuses on the back ground. Notably, there exists a Defocus Spread Effect along the boundary of the focus map. Due to this Defocus Spread Effect, an area surrounding the flower appears blurred in the source image 1. It is found that most of the methods do not perform well for this image pair. When observed carefully, it is seen that there is a blurred effect around the flower. There is no such effect occurs in the fused image generated by MIFED algorithm. This is due to edge superimposition.

The MIFED algorithm enhances the edges in the resultant image by superimposing the edges in the first source image on second source image and vice versa. Fusion is achieved by considering each and every element in the Dense SIFT feature vector of the corresponding pixels in the input images. Also, the algorithm combines the pixel and feature-based fusion technique, using the advantages of both methods.

5. CONCLUSION

The proposed approach tackles the depth of field issues through edge superimposition, employs Dense SIFT feature vector comparison for fusion and combines pixel and feature-based methods to enhance the object boundaries. The edges in the fused image get enhanced due to superimposition of edge details among the source images and extraction of orientation information in eight directions using dense SIFT descriptor. The level of feature extraction is high since Dense SIFT descriptor extracts feature vector for all pixels.

The picturesque quality of the fused image is good without any blurry or blocky artifact. The quantitative metrics AG, SF, EI and SD proves that most of the edge features are incorporated and better than all other methods considered.

The MIFED algorithm overcomes the optical lens depth of field problem, thereby making partially focused source images as a fully focused image. The MIFED algorithm can be used in automated systems such as robots to improve object detection and analysis particularly when the focus varies because of the distance from the camera. It can also be used in surveillance and security, when the images are captured in low lighting condition and helps to identify the objects or persons by improving the clarity of the source images. The MIFED algorithm works effectively for aligned images. If the source images are mis-aligned, then image registration should be done as a pre-processing step. In rare situation, the performance of the algorithm may be affected when the edge information is lacking in the corresponding location in both of the images.

In future, the MIFED algorithm can be extended with decision based fusion so as to improve Gradient-Based Similarity measurement and Phase Congruency. This extension can refine Gradient-Based Similarity measurement by consolidating gradients across different features or dimensions. Moreover, this enhancement can lead to more accurate identification and alignment of phase-related information, thereby improving the algorithm's ability to capture the underlying patterns and structures.

REFERENCES

[1] Z. Zhou, S. Li, and B. Wang, "Multi-scale weighted gradient-based fusion for multi-focus images," *Information Fusion*, Vol. 20, 2014, pp. 60–72.

[2] X. Fan, J. Zhang, M. Li, P. Shi, Bi. Zheng, X. Zhang, and Z. Yang, "A multi-sensor image fusion algorithm based on multi-scale feature analysis," *Proc. Int. Conf. IEEE IGARSS*, 2014, pp. 1623-1626.

[3] Y. Yang, D. S. Park, S. Huang, and N. Rao, "Medical image fusion via an effective wavelet-based approach," *EURASIP journal on advances in signal processing*, 2010, pp. 1-13.

[4] Y. Yang, S. Tong, S. Huang, and P. Lin, "Multifocus Image Fusion Based on NSCT and Focused Area Detection," *IEEE Sensors Journal*, Vol. 15, No. 5, 2015, pp. 2824-2838.

[5] S. Li, and B. Yang, "Multifocus image fusion using region segmentation and spatial frequency," *Image and Vision Computing*, Vol. 26, No. 7, 2008, pp. 971–979.

[6] H. Ying, and X. Rong, "A Block Image Fusion Algorithm Based on Algebraic Multi-grid Method," *Procedia Computer Science*, Vol. 131, 2018, pp. 273–281.

[7] Y. Zuo, J. Liu, G. Bai, X. Wang, and M. Sun, "Airborne Infrared and Visible Image Fusion Combined with Region Segmentation," *Sensors*, Vol. 17, No. 5, 2017, pp. 1127.

[8] R. Hang, Q. Liu, H. Song, and Y. Sun, "Matrix-based discriminant subspace ensemble for hyperspectral image spatial–spectral feature fusion," *IEEE Transactions on Geoscience and Remote Sensing*, Vol. 54, No. 2, 2016, pp. 783-794.

[9] S. Tello-Mijares, and J. Bescos, "Region-based multifocus image fusion for the precise acquisition of Pap smear images," *Journal of Biomedical Optics*, Vol. 23, No. 5, 2018, pp. 056005-056005.

[10] L. Xu, J. Hang, J. Han, T. Wang, and L. Bai, "Molten image fusion and enhancement based on image decomposition in frequency domain," *Signal, image and video processing*, Vol. 15, 2021, pp. 421-429.

[11] V. P. S. Naidu, and J. R. Raol, "Pixel-level image fusion using wavelets and principal component analysis," *Defence Science Journal*, Vol. 58, No. 3, 2008, pp. 338-352.

[12] R. Vijayarajan, and S. Muttan, "Discrete wavelet transform based principal component averaging fusion for medical images," *AEU-International Journal of Electronics and Communications*, Vol. 69, No. 6, 2015, pp. 896–902.

[13] M. B. A. Haghighat, A. Aghagolzadeh, and H. Seyedarabi, "Multi-focus image fusion for

visual sensor networks in DCT domain," *Computers and Electrical Engineering*, 2011, Vol. 37, No. 5, pp. 789–797. I. W. Selesnick, R. G. Baraniuk, and N. C. Kingsbury, "The dual-tree complex wavelet transform," *IEEE Signal Processing Magazine*, Vol. 22, No. 6, 2005, pp. 123-151.

[14] Y. Zhang, S. Wang, Y. Huo, L. Wu, and A. Liu, "Feature extraction of brain MRI by stationary wavelet transform and its applications," *Journal of Biological Systems*, Vol. 18, 2010, pp. 115–132.

[15] V. P. S. Naidu, "Image fusion technique using multi-resolution singular value decomposition," *Defence Science Journal*, Vol. 61, No. 5, 2011, pp. 479-484.

[16] S. Li, X. Kang, and J. Hu, "Image fusion with guided filtering," *IEEE Transactions on Image Processing*," Vol. 22, No. 7, 2013, pp. 2864-2875.

[17] S. Zheng, W. Z. Shi, J. Liu, G. X. Zhu, and J. W. Tian, "Multi source image fusion using support value transform," *IEEE Transactions on image processing*, Vol. 16, No. 7, 2007, pp. 1831-1839.

[18] B. K. Shreyamsha Kumar, "Multifocus and multispectral image fusion based on pixel significance using discrete cosine harmonic wavelet transform," *Signal, Image and Video Processing*, Vol. 7, 2013, pp. 1125-1143.

[19] A. Ellmauthaler, C. L. Pagliari, and E. A. Da Silva, "Multiscale image fusion using the undecimated wavelet transform with spectral factorization and nonorthogonal filter banks," *IEEE Transactions on Image Processing*, Vol. 22, No. 3, 2013, pp. 1005-1017.

[20] Y. Liu, X. Chen, H. Peng, and Z. Wang, "Multi-focus image fusion with a deep convolutional neural network," *Information Fusion*, Vol. 36, 2017, pp. 191–207.

[21] W. Zhao, D. Wang, and H. Lu, "Multi-focus image fusion with a natural enhancement via a joint multilevel deeply supervised convolutional neural network," *IEEE Transactions on Circuits and Systems for Video Technology*, Vol. 29, No. 4, 2018, pp. 1102–1115.

[22] H. Tang, B. Xiao, W. Li, and G. Wang, "Pixel convolutional neural network for multi-focus image fusion," *Information Sciences*, Vol. 433, 2018, pp. 125–141.

[23] Y. Yang, Z. Nie, S. Huang, P. Lin, and J. Wu, "Multilevel Features Convolutional Neural Network for Multifocus Image Fusion," *IEEE Transactions on Computational Imaging*, Vol. 5, No. 2, 2019, pp. 262-273.

[24] Y. Zhang, Y. Liu, P. Sun, H. Yan, X. Zhao, and L. Zhang, "IFCNN: A general image fusion framework based on convolutional neural network," *Information Fusion*, Vol. 54, 2020, pp. 99–118.

[25] X. Yan, S. Z. Gilani, H. Qin, and A. Mian, "Unsupervised deep multi-focus image fusion," *arXiv preprint arXiv:1806.07272*, 2018.

[26] B. Ma, X. Ban, H. Huang, and Y. Zhu, "Sesf-fuse: An unsupervised deep model for multi-focus image fusion," *arXiv preprint arXiv:1908.01703*, 2019.

[27] H. Jung, Y. Kim, H. Jang, N. Ha, and K. Sohn, "Unsupervised Deep Image Fusion With Structure Tensor Representations," *IEEE Transactions on Image Processing*, Vol. 29, 2020, pp. 3845-3858.

[28] H. Xu, J. Ma, Z. Le, J. Jiang, and X. Guo, "Fusiondn: A unified densely connected network for image fusion," *Proc. 34th AAAI Conference on Artificial Intelligence*, New York, 2020.

[29] A. Azarang, and N. Kehtarnavaz, "A generative model method for unsupervised multispectral image fusion in remote sensing," *Signal, Image and Video Processing*, Vol. 16, No. 1, 2022, pp. 63-71.

[30] P. Jagalingam, and A. V. Hegde, "A Review of Quality Metrics for Fused Image," *Science Direct Aquatic Procedia*, Vol. 4, 2015, pp, 133-142. doi:10.1016/j.aqpro.2015.02.019

[31] D. G. Lowe, "Distinctive Image Features from Scale-Invariant Keypoints," *International Journal of Computer Vision*, Vol. 60, No. 2, 2004, pp. 91-110.

[32] Y. Liu, S. Liu, and Z. Wang, "Multi-focus image fusion with dense SIFT," *Information Fusion*, Vol. 23, 2015, pp. 139-155.

[33] M. Abhyankar, A. Khaparde, and V. Deshmukh, "Spatial domain decision based image fusion using superimposition," *Proc. IEEE/ACIS 15th International Conference on Computer and Information Science*, Japan, 2016, pp. 1-6.

[34] X. Zhang, "Multi-focus image fusion.: A benchmark," *arXiv preprint arXiv:2005.01116*, 2020.

[35] S. Xu, X. Wei, C. Zhang, and J. Liu, J. Zhang, "MFFW: A new dataset for multi-focus image fusion," *arXiv preprint arXiv:2002.04780*, 2020.

[36] J. Zhang, Q. Liao, S. Liu, H. Ma, W. Yang, and J. H. Xue, "Real-MFF: A large realistic multi-focus image dataset with ground truth," *Pattern Recognition Letters*, Vol. 138, 2020, pp. 370-377.

H. Zhang, Z. Le, Z. Shao, H. Xu, and J. Ma, "MFF-GAN: An unsupervised generative adversarial network with adaptive and gradient joint constraints for multi-focus image fusion," *Information Fusion*, Vol. 66, 2020, pp. 40-53.

[37] B. K. Shreyamsha Kumar, "Image fusion based on pixel significance using cross bilateral filter," *Signal, Image and Video Processing*, Vol. 9, No.5, 2015, pp. 1193–1204.

[38] Y. Liu, X. Chen, R. K. Ward, and Z. Jane Wang, "Image Fusion With Convolutional Sparse Representation," *IEEE Signal Processing Letters*, Vol. 23, No. 12, 2016, pp. 1882-1886.

[39] X. Qiu, M. Li, L. Zhang, and X. Yuan, "Guided filter-based multi-focus image fusion through focus region detection," *Signal Processing: Image Communication*, Vol. 72, 2019, pp. 35–46.

[40] H. Ma, Q. Liao, J. Zhang, S. Liu, and J. H. Xue, "An α-Matte Boundary Defocus Model-Based Cascaded Network for Multi-Focus Image Fusion," *IEEE Transactions on Image Processing*, Vol. 29, 2020, pp. 8668-8679.

[41] Y. Liu, S. Liu, and Z. Wang, "A general framework for image fusion based on multi-scale transform and sparse representation," *Information Fusion*, Vol. 24, 2015, pp. 147–164.

[42] Y. Zhang, X. Bai, and T. Wang, "Boundary finding based multifocus image fusion through multi-scale morphological focus-measure," *Information Fusion*, Vol. 35, pp. 81–101, 2017.

[43] J. Ma, Z. Zhou, B. Wang, L. Miao, and H. Zong, "Multi-focus image fusion using boosted random walks-based algorithm with two-scale focus maps", *Neurocomputing*, Vol. 335, 2019, pp. 9–20.

Table 1: Feature based metrics of the existing methods and proposed method for lytro dataset

Method	AG	EI	$Q^{AB/F}$	Q_p	SD	SF
BFMF	6.84384	71.1102	0.73952	0.813292	61.3293	19.1835
BGSC	5.407235	55.5887	0.51773	0.463801	59.7947	15.9428
DSIFT	6.937035	72.0509	0.74481	0.818027	61.5838	19.4865
IFM	6.93147	71.9712	0.73629	0.793869	61.5121	19.4555
QB	6.929265	71.9706	0.74412	0.815647	61.5851	19.4827
TF	6.908155	71.7515	0.74542	0.819273	61.5533	19.409
ASR	6.778255	70.2154	0.72465	0.785958	60.9241	19.0673
CSR	6.83974	71.0839	0.73327	0.806346	61.4901	19.3217
CBF	6.726525	69.7607	0.73202	0.793537	60.9079	18.6761
DCT Corr	6.922705	71.9018	0.74033	0.805902	61.5017	19.427
DCT	6.932225	72.0009	0.74228	0.810574	61.5521	19.4608
DWTDE	6.7526	70.105	0.71635	0.78428	61.2544	18.9207
GD	6.89021	71.7468	0.67743	0.693197	57.3066	18.0243
MSVD	4.80397	49.543	0.50023	0.518228	58.9545	14.4333
MWGF	6.815705	70.8769	0.73247	0.809721	61.4692	19.2576
SVDDCT	6.92796	71.9542	0.74252	0.811085	61.555	19.4657
GFDF	6.902755	71.7009	0.74506	0.819468	61.5494	19.3971
GFF	6.89183	71.5529	0.74216	0.815251	61.4639	19.3473
MFM	6.89889	71.6534	0.74522	0.817426	61.5172	19.3682
MGFF	6.187375	64.4946	0.64478	0.677019	63.218	17.444
SFMD	8.153865	84.4034	0.64045	0.680628	62.9955	23.409
MST SR	6.93229	71.9989	0.73501	0.806941	61.7659	19.4452
NSCT SR	6.90897	71.7363	0.74146	0.814431	61.4384	19.4
RP SR	6.928545	71.8922	0.72029	0.77616	61.6498	19.5866
CNN	6.8752	71.4082	0.74425	0.818436	61.4954	19.299
DPRL	6.93919	72.0244	0.73773	0.817047	61.592	19.5194
ECNN	6.911405	71.7559	0.74102	0.805103	61.5804	19.4769
IFCNN	6.93388	71.9894	0.71278	0.771835	61.4441	19.4424
PCANet	6.88048	71.4715	0.73844	0.814058	61.551	19.3954
SESF	6.90953	71.7887	0.73987	0.811905	61.5881	19.4568
Proposed MIFED	9.96605	100.1881	0.739375	0.756797	63.9905	29.34379

(a1) (b1) (c1)

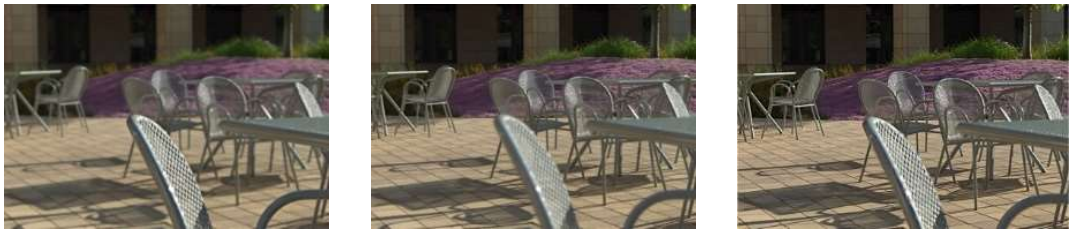

(a2) (b2) (c2)

(a3) (b3) (c3)

(a4) (b4) (c4)

(a5) (b5) (c5)

(a6) (b6) (c6)

Figure 2: Fusion results using proposed MIFED algorithm

Journal of Theoretical and Applied Information Technology
15th November 2025. Vol.103. No.21

ISSN: 1992-8645 www.jatit.org E-ISSN: 1817-3195

Figure 3: Fusion results using various methods and MIFED method